Applied Surface Science 433 (2018) 780–789

Contents lists available at ScienceDirect

Applied Surface Science

journal homepage: www.elsevier.com/locate/apsusc

Full length article

Theoretical study of the promotional effect of ZrO_2 on In_2O_3 catalyzed methanol synthesis from CO_2 hydrogenation

Minhua Zhang[a,b], Maobin Dou[a,b], Yingzhe Yu[a,b,*]

[a] Key Laboratory for Green Chemical Technology of Ministry of Education, R&D center for Petrochemical Technology, Tianjin University, Tianjin 300072, PR China
[b] Collaborative Innovation Center of Chemical Science and Engineering (Tianjin), Tianjin 300072, PR China

ARTICLE INFO

Article history:
Received 10 July 2017
Received in revised form
12 September 2017
Accepted 13 October 2017
Available online 17 October 2017

Keywords:
CO_2 hydrogenation
Methanol synthesis
In_2O_3
ZrO_2
HCOO route
DFT

ABSTRACT

Methanol synthesis from CO_2 hydrogenation on the ZrO_2 doped $In_2O_3(110)$ surface (Zr-$In_2O_3(110)$) with oxygen vacancy has been studied using the density functional theory calculations. The calculated results show that the doped ZrO_2 species prohibits the excessive formation of oxygen vacancies and dissociation of H_2 on In_2O_3 surface slightly, but enhances the adsorption of CO_2 on both perfect and defective Zr-$In_2O_3(110)$ surface. Methanol is formed via the HCOO route. The hydrogenation of CO_2 to HCOO is both energetically and kinetically facile. The HCOO hydrogenates to polydentate H_2CO (p-H_2CO) species with an activation barrier of 0.75 eV. H_3CO is produced from the hydrogenation of monodentate H_2CO (mono-H_2CO), transformation from p-H_2CO with 0.82 eV reaction energy, with no barrier whether there is hydroxyl group between the mono-H_2CO and the neighboring hydride or not. Methanol is the product of H_3CO protonation with 0.75 eV barrier. The dissociation and protonation of CO_2 are both energetically and kinetically prohibited on Zr-$In_2O_3(110)$ surface. The doped ZrO_2 species can further enhance the adsorption of all the intermediates involved in CO_2 hydrogenation to methanol, activate the adsorbed CO_2 and H_2CO, and stabilize the HCOO, H_2CO and H_3CO, especially prohibit the dissociation of H_2CO or the reaction of H_2CO with neighboring hydride to form HCOO and gas phase H_2. All these effects make the ZrO_2 supported In_2O_3 catalyst exhibit higher activity and selectivity on methanol synthesis from CO_2 hydrogenation.

1. Introduction

The efforts to mitigate global climate change through catalytic conversion of CO_2 into methanol, which has been widely used as hydrogen energy carriers and the feedstock for the production of many other chemicals, has attracted considerable interest utilizing heterogeneous metal and metal oxide catalysts [1–4]. The formate (HCOO) route, the reverse water gas shift (RWGS) route, and the hydrocarboxyl (COOH) route are the three reaction pathways which had been proposed for methanol synthesis from CO_2 hydrogenation on the extensively studied Cu-based and Pd-based metal catalysts through both experiments and theory [5–10]. The CO_2 is firstly converted to HCOO which is followed by a consecutive hydrogenation from dioxymethylene (H_2COO), methoxy (H_3CO) to the product methanol (CH_3OH) in the HCOO route.

Compared with the lower methanol selectivity of CO_2 hydrogenation on Cu-based and Pd-based catalysts, the metal oxide catalysts, In_2O_3 catalyst has shown superior catalytic performance with higher methanol selectivity and space time yield [11]. In the methanol [12] and ethanol [13] steam reforming reactions, the In_2O_3 catalysts show near 100% CO_2 selectivity for the suppression of reverse water-gas shift (RWGS) reaction. Bielz et al. found that CO can easily reduce the In_2O_3, while CO_2 can't replenish the oxygen vacancy. Whereas CO_2 evolution via reaction of a $CO + H_2O$ mixture on In_2O_3 above 430 K, only trace amounts of CO are found upon reaction in a $CO_2 + H_2$ mixture [14]. Sun et al. reported that adsorbed CO_2 on In_2O_3 surface is more highly activated than on the Ga_2O_3 surface, and confirmed that In_2O_3 is a promising catalyst for CO_2 conversion reactions [15]. The experimental results of Sun et al. demonstrated that the temperature and pressure have a significant effect on methanol yield of CO_2 hydrogenation and the products are only CO and methanol, whose yield is higher than that of many other reported catalysts [16]. Martin et al. unveiled

---

* Corresponding author at: Key Laboratory for Green Chemical Technology of Ministry of Education, R&D center for Petrochemical Technology, Tianjin University, Tianjin 300072, PR China.
E-mail address: yzhyu@tju.edu.cn (Y. Yu).

https://doi.org/10.1016/j.apsusc.2017.10.097
0169-4332/© 2017 Elsevier B.V. All rights reserved.

that the In_2O_3-based catalyst has the performance of high activity, 100% methanol selectivity and remarkable stability under industrially relevant conditions for CO_2 hydrogenation, which strongly contrasts to the benchmark Cu-ZnO-Al_2O_3 catalyst [11]. The theoretical research of CO_2 hydrogenation on In_2O_3 surface by Ye et al. revealed that the oxygen vacancy on In_2O_3 surface is the pivotal site for CO_2 adsorption and activation [17,18]. The perfect In_2O_3 surface firstly reacts with hydrogen to form oxygen vacancy and then adsorbs CO_2 with one of the oxygen atom filling the oxygen vacancy. This is followed by a consecutive hydrogenation of the activated CO_2 to produce methanol according to the HCOO reaction pathway. The experimental results also indicated that the oxygen vacancy is the active site on In_2O_3 catalyst which has higher activity when pre-activated using CO as reducing agent [11]. Besides, the ZrO_2 supported In_2O_3 catalyst shows higher methanol yield than pure In_2O_3 catalyst at the same conditions. The reason, the authors thought, for the promotional effect of ZrO_2 on In_2O_3 catalyst is that ZrO_2 can promote the formation of oxygen vacancy on In_2O_3 surface, which leads to the increasing number of active sites and methanol yield. While it can not be excluded that the oxygen vacancies contained in ZrO_2 itself, which is nonactive, resulted in the increasing of oxygen vacancy. Therefore, more detailed studies are needed to reveal the exact interaction between ZrO_2 support and In_2O_3 catalyst. The experimental [19–21] and theoretical [22–24] studies on Cu/ZrO_2 catalyst for CO_2 hydrogenation indicated that the interaction between Cu and ZrO_2 species has a crucial effect on the activity and methanol selectivity. In the interface between Cu and ZrO_2 species, the Zr^{4+} is partially reduced to Zr^{3+} (or formation of oxygen vacancy) which is able to bind the key intermediates e.g. $CO_2{}^*$, CO^*, HCO^* and H_2CO^*, moderately to facilitate the formation of methanol. The phenomenon that Zr^{4+} is partially reduced to Zr^{3+} on ZrO_2 is also observed by Martin [11] et al. at the interface between In_2O_3 and ZrO_2 species. Compared with the interaction between ZrO_2 and Cu species, does the interaction between ZrO_2 and In_2O_3 species just promote the formation of oxygen vacancy on In_2O_3 surface?

In present work, we examine the influence of doped ZrO_2 on the property of In_2O_3 and methanol synthesis from CO_2 hydrogenation using density functional theory (DFT). We first compared the difference between pure In_2O_3 and ZrO_2-doped In_2O_3 (Zr-In_2O_3) on oxygen vacancy formation and CO_2 and H_2 adsorption, and then mapped out the route for methanol synthesis from CO_2 hydrogenation on Zr-In_2O_3 surface. Finally, we compared the difference of the adsorption of key intermediates between pure and ZrO_2-doped In_2O_3 surface.

2. Computational details

All the DFT calculation were carried out with the program package Dmol^3 in Materials Studio of Accelrys Inc [25,26]. The generalized gradient approximation (GGA) with Perdew-Burke-Ernzerhof functional was utilized to account for the exchange and correlation effects [27]. The basis set was set as double numerical plus polarization (DNP). The basis set superposition error (BSSE) calculation was not performed in this paper since it is very small and can be neglected [28]. To take the relativity effect into account, the density functional semicore pseudopotential (DSPP) method was employed for the In and Zr atoms with spin-unrestricted calculations, and the other atoms were treated with the all electron basis set. A Fermi smearing of 0.001 Ha was adopted to accelerate the convergence and a $2 \times 2 \times 1$ grid was used to generate k-points according to the Monkhorst-Pack method [29]. The convergence criteria for geometry optimization and energy calculation were set as 1.0×10^{-6} Ha, 1.0×10^{-5} Ha, 0.002 Ha Å^{-1}, and 0.005 Å for the tolerance of self-consistent field (SCF), energy, maximum force, and maximum displacement, respectively.

The perfect $In_2O_3(110)$ surface was modeled with a $(1 \times \sqrt{2})$ supercell, built from the optimized In_2O_3 bulk unit [17,18,30] shown in Fig. 1a. The supercell has a dimension of 14.54×10.28×18.03 Å. The ZrO_2 doped $In_2O_3(110)$ surface was modeled by substituting the two adjacent surface In_1 and In_2 atoms in the In-O chain as Fig. 1c shows. The oxygen vacancy on the (Zr-)$In_2O_3(110)$ surface was created through removing one surface O atom from the perfect (Zr-)$In_2O_3(110)$ surface. In all calculations, the bottom two layers were fixed at their equilibrium bulk positions, whereas the top two layers together with the adsorbates were allowed to relax. The adsorption energy of adsorbates, E_a, was defined as given in Eq. (1)

$$E_a = E_{A/S} - E_A - E_S \qquad (1)$$

Where A represents absorbate and S represents the perfect or defective $In_2O_3(110)$ surface and Zr-$In_2O_3(110)$ surface slab. $E_{A/S}$, E_A, and E_S represent the total energies of the surface slab with the adsorbates, the isolated molecule (radical), and the clean optimized perfect Zr-$In_2O_3(110)$ surface and the defective Zr-$In_2O_3(110)$ sur-

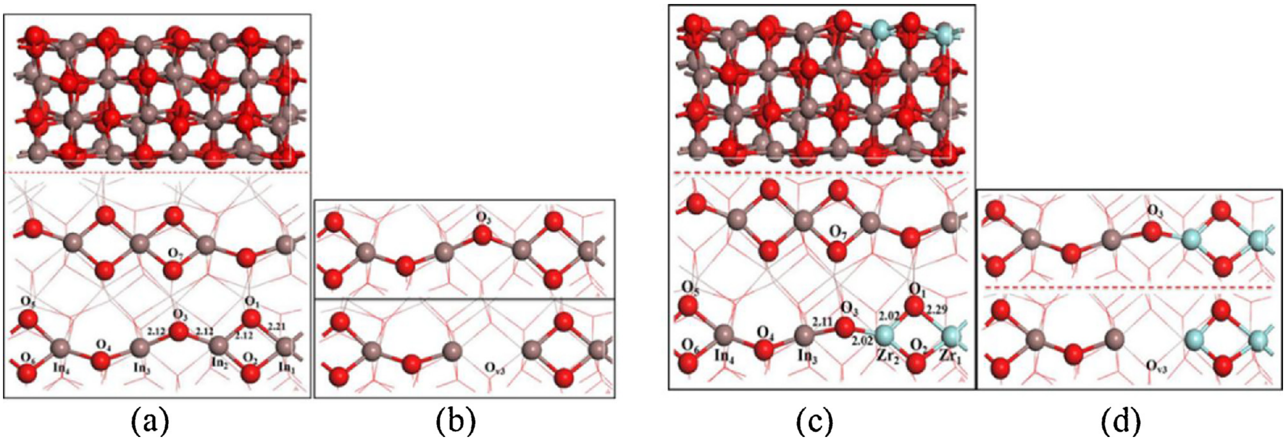

Fig. 1. (a) The optimized structure of the $In_2O_3(110)$ surface, side view (upper) and top view (lower). (b) The optimized structure before (upper) and after (lower) the creation of O_{v3} vacancy on $In_2O_3(110)$ surface. (c) Optimized structure of the Zr-$In_2O_3(110)$ surface. (d) The optimized structure before and after the creation of O_{v3} vacancy on Zr-$In_2O_3(110)$ surface. Red, O atoms; brown, In atoms; Cyan, Zr atoms. (For interpretation of the references to colour in this figure legend, the reader is referred to the web version of this article.)